Title

Assessing Variant Causality and Severity Using Retinal Pigment Epithelial Cells Derived from Stargardt Disease Patients

Journal

Translational Vision Science & Technology, 11(3)

ISSN

2164-2591

Authors

Matynia, Anna
Wang, Jun
Kim, Sangbae
et al.

Publication Date

2022-03-29

DOI

10.1167/tvst.11.3.33

Peer reviewed

tvst

Article

Assessing Variant Causality and Severity Using Retinal Pigment Epithelial Cells Derived from Stargardt Disease Patients

Anna Matynia[1], Jun Wang[2,3], Sangbae Kim[2,3], Yumei Li[2,3], Anupama Dimashkie[4], Zhichun Jiang[1], Jane Hu[1], Samuel P. Strom[5], Roxana A. Radu[1], Rui Chen[2,3,6], and Michael B. Gorin[1]

[1] UCLA Stein Eye Institute and Department of Ophthalmology, David Geffen School of Medicine, University of California, Los Angeles, CA, USA
[2] Human Genome Sequencing Center, Baylor College of Medicine, Houston, TX, USA
[3] Department of Molecular and Human Genetics, Baylor College of Medicine, Houston, TX, USA
[4] Eli and Edythe Broad Stem Cell Research Center, University of California, Los Angeles, CA, USA
[5] Fulgent Genetics, Santa Anita, CA, USA
[6] Structural and Computational Biology and Molecular Biophysics Graduate Program, Baylor College of Medicine, Houston, TX, USA

Correspondence: Anna Matynia, Stein Eye Institute, Department of Ophthalmology, David Geffen School of Medicine, University of California, 10833 Le Conte Avenue, Los Angeles, CA 90095, USA.
e-mail: matynia@jsei.ucla.edu

Received: December 6, 2021
Accepted: February 19, 2022
Published: March 29, 2022

Keywords: induced pluripotent stem cells; retinal pigment epithelium; Stargardt disease; macular degeneration; molecular genetics; mutation; transcriptome; allele specific imbalance; genotype-phenotype correlation

Citation: Matynia A, Wang J, Kim S, Li Y, Dimashkie A, Jiang Z, Hu J, Strom SP, Radu RA, Chen R, Gorin MB. Assessing variant causality and severity using retinal pigment epithelial cells derived from Stargardt disease patients. Transl Vis Sci Technol. 2022;11(3):33, https://doi.org/10.1167/tvst.11.3.33

Purpose: Modern molecular genetics has revolutionized gene discovery, genetic diagnoses, and precision medicine yet many patients remain unable to benefit from these advances as disease-causing variants remain elusive for up to half of Mendelian genetic disorders. Patient-derived induced pluripotent stem (iPS) cells and transcriptomics were used to identify the fate of unsolved *ABCA4* alleles in patients with Stargardt disease.

Methods: Multiple independent iPS lines were generated from skin biopsies of three patients with Stargardt disease harboring a single identified pathogenic *ABCA4* variant. Derived retinal pigment epithelial cells (dRPE) from a normal control and patient cells were subjected to RNA-Seq on the Novaseq6000 platform, analyzed using DESeq2 with calculation of allele specific imbalance from the pathogenic or a known linked variant. Protein analysis was performed using the automated Simple Western system.

Results: Nine dRPE samples were generated, with transcriptome analysis on eight. Allele-specific expression indicated normal transcripts expressed from splice variants albeit at low levels, and missense transcripts expressed at near-normal levels. Corresponding protein was not easily detected. Patient phenotype correlation indicated missense variants expressed at high levels have more deleterious outcomes. Transcriptome analysis suggests mitochondrial membrane biodynamics and the unfolded protein response pathway may be relevant in Stargardt disease.

Conclusions: Patient-specific iPS-derived RPE cells set the stage to assess non-expressing variants in difficult-to-detect genomic regions using easily biopsied tissue.

Translational Relevance: This "Disease in a Dish" approach is likely to enhance the ability of patients to participate in and benefit from clinical trials while providing insights into perturbations in RPE biology.

Introduction

The advent of modern molecular genetic analyses has revolutionized genetic diagnoses, from gene discovery to diagnostics to assignment of causality. Genome sequencing, population-based databases, annotation, genotype-phenotype correlations have greatly increased how many patients know their molecular details and can fully participate in all levels of clinical care, including clinical trials and precision or personalized medicine. Yet, there remains up to 30% of patients without a complete molecular genetics diagnosis for inherited retinal diseases (IRDs).[1–3] The genome still has "dark DNA" that may harbor as-yet-undiscovered causative variants due to difficult-to-sequence or inability to assign causation to noncoding regions with low conservation.[4] Epigenetic effects, digenic or multigenic diseases, the presence or absence of hypomorphic alleles, and gene-environment interactions all further complicate molecular genetics diagnoses.

Stargardt disease is a macular dystrophy that is genetically heterogeneous but for which more than 90% of cases can be attributed to an autosomal recessive disorder involving pathogenic variants in *ABCA4*.[5–7] Clinical molecular diagnosis has undergone rapid advances in targeted genomic sequencing of the 50 exons and splice sites, and development of databases with over 2000 exonic and intronic variants in *ABCA4* (https://databases.lovd.nl/shared/variants/ABCA4/). The identification of novel pathogenic variants has also expanded significantly over the past 5 to 10 years as the percentage of patients with only a single or no identified variants decreased from approximately 50% to 30% currently,[8–10] enabling clinicians to recognize a much broader range of phenotypes for ABCA4-related retinopathies than the original clinical description by Stargardt.[7] Clearly, large gaps remain in our ability to identify novel variants that will allow all patients to have a complete molecular diagnosis.

ABCA4 is only expressed in the retinal pigment epithelium (RPE) and photoreceptor cells, excluding the practicality of tissue biopsy.[11,12] Splice and promoter variants are often identified by in silico analyses requiring validation of altered gene expression ex vivo or when biopsied tissue is not available, in vitro. In Stargardt disease, such mini- and midi-gene assays have been used to verify altered gene expression and often are used to classify variants as mild, moderate, or severe alleles.[13–15] Although critical to validating variants, these methods are unable to detect global contributions to expression by distal genetic elements and cellular factors with respect to transcription and mRNA processing.

To gain insight into the fate of the putative normal allele of patients with a single identified *ABCA4* variant, patient-derived RPE generated from skin biopsies via induced pluripotent stem (iPS) cells was analyzed for *ABCA4* expression. The ability to differentiate numerous cells types from patient-derived iPS cells removes the burden of risky biopsies and provides plentiful personalized tissue samples for not just transcriptomic but a large variety of probative assays. This "Disease in a Dish" approach can be done on single-cell type cultures, from which RPE cells can be easily derived,[16–19] or in mini organs, from which photoreceptor precursors can be derived.[18,20–26] In these studies, patient-derived iPS cells were differentiated into RPE (dRPE) cells and the transcriptional consequences from unidentified *ABCA4* variants of clinically diagnosed patients with Stargardt disease with only a single solved allele were explored.

Methods

Patient Recruitment

All three individuals were recruited and enrolled in the Genetics research study with approval of the UCLA Institutional Review Board (IRB) and in accordance with regulations of the Health Insurance Portability and Accountability Act of 1996 (HIPAA), with signed informed consent after explanation of the nature and possible consequences of the study and specifying the use of the information for publications and research presentations. DNA samples were obtained from saliva or whole blood specimens and fibroblasts from skin biopsies using standard protocols.

Variant Validation

Genomic DNA was isolated using an automated system (Chemagen, Perkin Elmer) or QIAmp kits (Qiagen), total RNA using RNeasy (Qiagen), and cDNA prepared using the High-Capacity cDNA Reverse Transcription Kit (Applied Biosystems). Single band polymerase chain reaction (PCR) amplification with Taq polymerase (Bioland Scientific; C1000 Touch, Bio-Rad) was verified and subjected to Sanger sequencing (Laragen, Inc., Culver City, CA). Sequence alignment and variant detection were performed using Sequencher (Gene Codes Corp.). Star reagents are listed in Supplementary Table SA1 and primer sequences in Supplementary Table SA2.

Generation of iPS and dRPE Cells

All tissues/cells were processed in a certified BSL-2 Biological Safety Cabinet (BSC) and incubated at 37°C in 5% CO_2 with filter sterilized media stored no longer than 7 days at 4°C unless otherwise specified.

Fibroblast: Punch biopsies were immersed in Dulbecco's modified Eagle's medium (DMEM)/F12 and transferred under aseptic conditions to the UCLA manufacturing facility. Biopsies were rinsed in DMEM/F12 media, chopped into 1-mm pieces and incubated in 1 mg/mL animal origin free collagenase for 1 hour. Tissue was collected by centrifugation at 300 x*g* for 5 minutes, the supernatant aspirated, and the pellet washed with 10 mL of serum-free mesenchymal stem cell growth medium-chemically defined (MSCGM-CD) and centrifuged as above. Pellets containing the dissociated cells and tissue clumps were resuspended in MSCGM-CD medium and plated on a CELLstart-coated (Invitrogen) dish using Fibrogro medium (Millipore) with 1X antibiotic/antimycotic. The medium was changed once every 72 hours until the cell monolayer was 70% confluent, and the cells passaged using TrypLE (Invitrogen). Single-cell suspensions were cryopreserved in ProFreeze CDM (Lonza), as per the manufacturer's protocol.

iPS: Patient-specific fibroblasts were thawed at 37°C, resuspended in Fibrogro media (Millipore), and checked for cell viability using trypan blue. Cells were centrifuged as above, resuspended in mTESR1 (serum- and feeder-free; Stem Cell Technologies) media with 1X antibiotic/antimycotic (Thermofisher), plated at 100,000 cells per well and incubated overnight. Cells were reprogrammed using the Simplicon RNA Reprogramming kit (Millipore) per the standard operating protocol for 4 to 6 weeks. The iPS cell colonies were replated using ReLeSR (Stem Cell technologies), and passaged with daily media changes until iPS cell stabilization at passage 7 to 10. Single-cell suspensions were cryopreserved in ProFreeze CDM (Lonza), as per the manufacturer's protocol. The iPS cells were propagated in mTeSR media with 5 times supplements (Stem Cell Technologies) on Matrigel coated tissue culture plates, and passaged using ReLeSR.

dRPE: Reprogramming of iPS cells into dRPE was performed in triplicate for each line using the Buchholtz method,[27] by culturing for 2 days each in DMEM/F12 medium with Glutamax, NEAA, B27, N2, and: 50 ng/mL Noggin, 10 ng/mL Dkk1, and 10 ng/mL IGF1 (days 1–2); 10 ng/mL Noggin, 10 ng/mL Dkk1, 10 ng/mL IGF1, and 5 ng/mL bFGF (days 3–4); 10 ng/mL Dkk1 and 10 ng/mL IGF1 (days 5–6); 100 ng/mL Activin A and 10 µM Su-5402 (days 7–14) then maintained on αMEM with Glutamax, NEAA, N1, 50 mg/mL taurine, hydrocortisone, Triiodo-thyroxin, and 5% fetal bovine serum (FBS). The dRPE pigmented colonies were picked, dissociated with 0.25% Trypsin/EDTA for 10 minutes at 37°C with inversion, and triturated. Media with FBS was added, centrifuged as above, cells counted, and passaged onto laminin coated plates with fresh medium. Differentiation was visualized by the cobblestone morphology, pigmentation, dRPE specific gene expression and transepithelial resistance. P2 cultures were harvested after a minimum of 75 days in culture. Pigmented cells were manually counted using FIJI/ImageJ. The ellipsoid tool was used to select that area of interest in 8-bit images, the outside cleared, the threshold adjusted to show white areas prominently, a dark background applied, and the image made binary and inverted. A Freehand tool was used to select pigmented or non-pigmented RPE, and the areas measured and exported to an Excel spreadsheet.

Protein Analysis

Capillary electrophoresis was performed on the fully automated Simple Western system (Wes by Protein Simple, San Jose, CA) per manufacturer's protocol. Briefly, 20 µg of total protein dRPE cell homogenates were heat-denatured in DTT, added to the assay plate containing blocking buffer, primary and secondary antibody and wash buffer, and separated on the 66 to 440 kDa Wes separation cartridge with goat anti-human ABCA4 (1:25, EB08615, Everest Biotech Ltd.) as a primary antibody and HRP-conjugated secondary anti-goat antibody for detection. Retinal homogenates (20 µg) from wild type and *ABCA4* knock out mice served as positive and negative protein controls, respectively. Gel images were obtained using the WES system software.

Transcriptome Analysis

All transcripts were aligned with the reference genome hs:19. RNASeq (50 million reads per sample on Novaseq6000 from Illumina), raw data was converted to fastq, mapped using STAR Aligner, transcript estimation using Cufflink (FPKM and HTseq2 for read counts). Data analysis was performed with the quality control normalization using the DESeq2 package, clustering and principal component analysis, and differential gene expression. Allele specific imbalance (ASI) was calculated as the percentage of total gene expression in Transcripts Per Kilobase Million (TPM) by the ratio of count for the alternate (variant 1) and reference (normal) nucleotide at

the respective locations for each patient. Statistical analysis was performed using the ANOVA testing and MAANOVA package.

Results

Patient Characterization

Three patients with a single confirmed heterozygous ABCA4 pathogenic allele (variant 1, Table 1) and an allele with no previously detected pathogenic variants despite a clinical diagnosis of Stargardt disease were recruited. During the study, the unsolved pathogenic alleles for two of these participants were identified (variant 2, Table 1).[4] Autofluorescence fundus imaging revealed classic geographic atrophy in the macula surrounded by autofluorescence in all three patients (Figure 1).

Patient 1: (H) A man, disease onset at approximately 26 years old with reduced best-corrected visual acuities (BCVA) with light sensitivity but no night blindness or gross color discrimination deficits. Ocular examination revealed the following: BCVA 20/160 OD and 20/200 OS; intraocular pressure (IOP) on last visit 18 OD and 18 OS; optical coherence tomography (OCT) and fundus autofluorescence (FAF) showed central outer retinal thinning with scattered hyper autofluorescent deposits, incomplete geographic atrophy with limited foveal preservation consistent with moderate Stargardt disease; rod isolated and maximal, and cone isolated and 30 Hz cone flicker electroretinographic responses were generally within normal limits. Previous genetic testing included mutation screening in: *ELOVL4*, *RP1*, *PRPH2*, and *ABCA4*. The only variant identified was in *ABCA4*: c.3386G>T, p. R1129L, (chr1:94506901). During the course of this study, whole exome sequencing (WES) and single-molecule molecular inversion probes (smMIPs) analyses confirmed the missense variant and identified a second splice variant in cis with a hypomorphic allele in *ABCA4*[10,28]: c.5461-10T>C; c.5603A>T, p.[Thr1821Aspfs*6,Thr1821Valfs*13; Asn1868Ile], chr1:94476951.[4]

Patient 2: (J) A woman, disease onset at approximately 40 years old with reduced BCVAs and paracentral scotomas. Ocular examination revealed the following: BCVA 20/60 OD and 20/100 OS; IOP on last visit 14 OD and 17 OS; OCT and FAF showed central outer retinal thinning and scattered hyper autofluorescent deposits in the posterior pole, and incomplete central geographic atrophy consistent with mild Stargardt disease; electroretinography was not performed. Previous genetic testing included mutation screening in: *ABCA4*, *BEST1*, *CDH23*, *EFEMP1*, *ELOVL4*, *IMPG1*, *IMPG2*, *PROM1*, *RDS*, and *TIMP3*. The only pathogenic variant identified was in *ABCA4*: c.570+1798A>G, p.PE, chr1:94566773 insertion. During the course of this study, whole genome sequencing (WGS) and smMIPs analyses confirmed the known splice variant and failed to identify a second pathogenic variant.[4]

Table 1. *ABCA4* Pathogenic Variants in Participants

Variant 1	Variant 2	Cell Line	Disease Severity	Variant Class[a]	No. of Cell Lines
c.3386G>T; p.R1129L	c.5461+10T>C; splice site	H	Moderate	Severe	2
c.570+1798A>G; splice site	Unsolved	J	Mild	Severe	3
C.3364G>A; p.E1122K	c.2654-8T>G; splice site	S	Moderate-severe	Severe	3
None	None	Control	N/A	N/A	1

[a]Midi-gene expression classification[4].
N/A, not applicable.

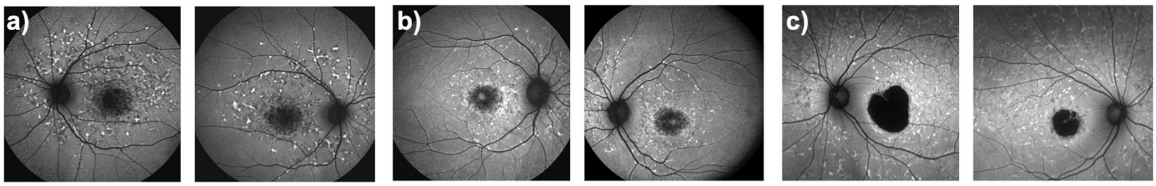

Figure 1. Macular degeneration is observed in fundus images of each patient participant. (**a**) H with moderate Stargardt's disease, (**b**) J with mild Stargardt's disease, and (**c**) S with moderate to severe Stargardt's disease, have characteristic geographic atrophy and autofluorescence observed in and surrounding the macula, respectively, indicative of macular degeneration. Age at fundus imaging and BCVA, respectively: H = 39 and 39; J = 58 and 62: and S = 35 and 35.

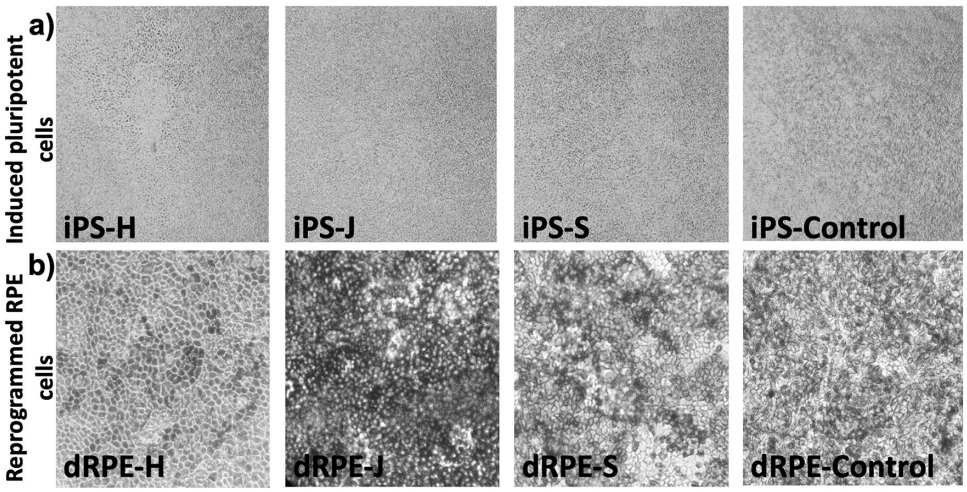

Figure 2. Pigmented, cobblestone dRPE cells were reprogrammed from iPS cells. Representative cultures for a single line from each patient show (**a**) iPS cells prior to differentiating into RPE cells and (**b**) pigmented cobblestone dRPE cells prior to harvest after 3 months in culture.

Patient 3: (S) A woman, disease onset at approximately 13 years old with central vision loss that was not correctable by refraction. Ocular examination revealed the following: BCVA 20/200 OD and 20/200 OS; IOP on last visit 15 OD and 15 OS; OCT and FAF showed central outer retinal thinning and subRPE deposits with diffuse hyper autofluorescence of the RPE as well as numerous hyper autofluorescent deposits in the posterior pole and extensive geographic atrophy consistent with moderate to severe Stargardt disease; rod isolated and maximal, and cone isolated and 30 Hz cone flicker electroretinographic responses were within normal limits. Previous genetic testing included mutation screening in: *PRPH2*, and *ABCA4*. The only pathogenic variant identified was in *ABCA4*: c.3364G>A, p. E1122K, chr1:94506923. During the course of this study, sequencing and smMIPs analyses confirmed the missense variant and a second splice variant was identified in *ABCA4*: c.2654-8T>G, p.[40-nt e18 elongation,=], chr1:94517225.[4]

dRPE Cell Generation and Characterization

The dRPE cells were reprogrammed for each of three independent iPS lines of every patient by standard procedures.[27] Growth and maturation (assessed by pigmentation) were similar (Figure 2), and transepithelial resistance in the range of 150 to 250 Ω/cm^2 indicated proper tight junction formation in representative samples.[17] One "H" iPS line failed to reprogram into confluent cultures of pigmented dRPE cells and was not further analyzed. The percentage of dRPE (pigmented and unpigmented) cells in each culture ranged from 99.5% to 100% except for a J2, which contained 81.6% dRPE and was not further analyzed. The percentage of pigmented and all dRPE cells for each patient was: 98.8 ± 0.4% and 99.9 ± 0.1% (H); 96.3 ± 1.8% and 100.0 ±0.0% (J); 95.0 ± 2.4% and 99.8 ± 0.2% (S); and 94.0 ± 5.9% and 100.0 ± 0.0% (control). Patient variants were confirmed in these dRPE cells at this time.

Allele Specific Imbalance and Expression Indicate Normal Transcripts Generated from Splice Variants

ASI was assessed from the nucleotide count at the variant 1 locus from five million reads of RNASeq data. For the H and S lines with their respective missense variants, readthrough of the splice variants (Ref) represents 16.53% and 27.96% of total transcripts, with the control lines expressing only the normal transcript (Figure 3). In the J lines, the relative expression of the splice and unknown was determined by segregation analysis with a heterozygous polymorphism in exon 49. The severe splice variant (c.570+1798A>G) represents 14.21% of total transcripts.

ABCA4 expression was 68% (H), 28% (J), and 165%(S) relative to the NHFD controls, representing the combined missense and splice variant transcripts. Replicates of the S line had expression levels that ranged from 98% to 286% of control, however, the

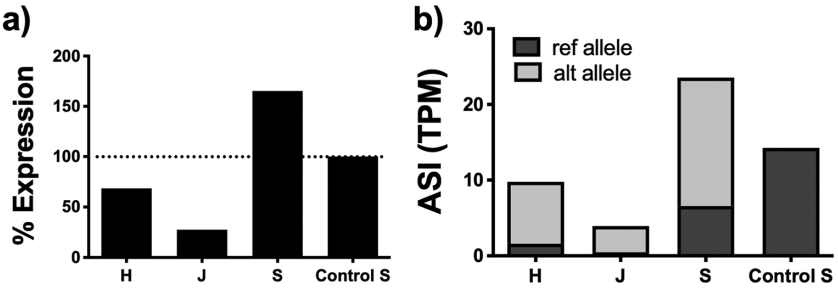

Figure 3. **ABCA4 has altered expression and hypomorphic splice variants in patient dRPE cells.** (**a**) The level of expression relative to the control dRPE cells shows decreased expression in two patient lines (H, J) and increased expression in one patient line (S). The total expression in the each independently derived line was similar or higher than the control: S1 (16.0 TPM), S2 (40.8 TPM), and S3 (13.9 TPM). (**b**) Allele specific imbalance (ASI), determined as the count for each nucleotide at the known variant locus. All patient lines have significantly reduced expression of variant 1 (Alt, Table 1) where variant 1 is their respective missense variants for H and S, and the solved splice variant for J.

Table 2. *ABCA4* mRNA Relative Expression

			ASI at Variant 1		
Sample	TPM – *ABCA4*	% Expression[a]	TPM - Ref[b]	TPM - Alt[b]	% Ref Expression[c]
H	9.78	68.5	1.62	8.16	11.3
J	3.94	27.6	3.38	0.56	23.7
S	23.58	165.1	6.59	16.99	46.1
Control	14.28	100	14.28	n/a	n/a

[a]Total expression of combined variant and normal alleles.
[b]Allele specific expression of normal (Ref) and variant 1 alleles indicating imbalance.
[c]Expression of normal allele (Ref) relative to control.

relative level of each allele was similar. The percent of transcript attributable to readthrough of the splice variants (Ref) is reduced in all patient lines, albeit only slightly for the S lines, compared to unbiased expression (Table 2).

Transcriptome Alterations in Stargardt Disease dRPE Cells

Principal component analysis showed clear distinctions among the three patient and control dRPE transcriptomes (Appendix Figure 1). Analysis of differentially expressed genes (DEGs) identified 221 DEGs in patient versus control dRPE transcriptomes. Clustering of the top 50 DEGs shows clear distinctions between patient and control dRPE transcriptomes (Figure 4A). There were 35 DEGs that had statistically significant changes (see Figure 4B, $P < 0.001$), and represent broad biological functions, including transcription, metabolism of nucleotides, protein and lipids, ion transport, and cell adhesion and signaling. Pathway analysis identified mitochondrial structure or function as potentially disrupted. Eight of 111 genes in the Unfolded Protein Response pathway were identified as DEGs that could be activated by both missense and splice variants generating short-lived protein isoforms (see Figure 4C, $P < 0.05$).

Patients with Stargardt Disease dRPE Cells have Varying Levels of ABCA4 Protein

Protein levels of pABCA4 were determined by Western blot analysis using the automated WES system for low abundance proteins. The pABCA4 protein was detected in all lines but at strongly reduced levels and as truncated proteins or degradation products except S2, compared to the control (Figure 5), consistent with mRNA expression levels. In agreement with increased expression of *ABCA4* mRNA, the S2 line appears to have relatively normal pABCA4 levels and molecular weight in the range of modified, mature membrane protein.

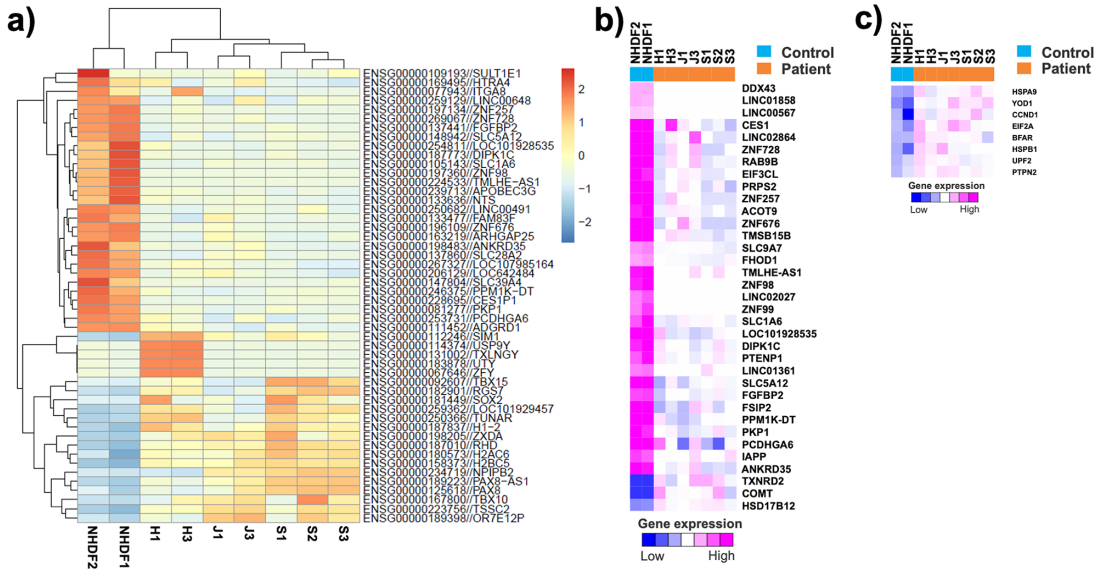

Figure 4. **Transcriptome analysis highlights disease-specific changes.** (**a**) Clustering of top 50 DEGs indicate clear differences in patient dRPE transcriptomes compared to controls and potential personalized transcriptome alterations. (**b**) 35 genes had significant expression level differences ($P < 0.001$) out of 221 identified DEGs. (**c**) Eight genes involved in the unfolded protein response had significant expression level differences ($P < 0.05$) out of 111 identified DEGs.

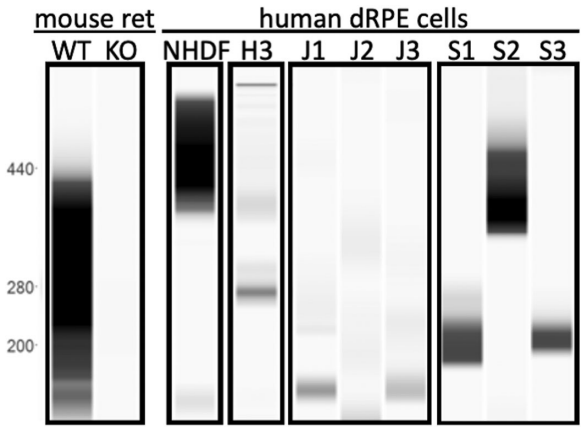

Figure 5. **The pABCA4 is expressed in patient dRPE cells.** Mouse retina (mouse ret) contains abundant pAbca4 in wild type (WT) and no protein in *Abca4* knockout (KO) mice. The human control (NHDF) has abundant protein with a higher apparent molecular weight than WT mouse retina. All patient dRPE cells (H, J, and S) show low abundance of pABCA4 protein that is likely degraded, indicated by the decreased molecular size. Molecular size markers are indicated on the left.

Discussion

Analysis of patient tissue biopsies can greatly synergize with in vivo imaging and functional assessment, along with other in vivo assessments for the diagnosis, prognosis, and clinical treatment of disease. When the cell types affected by disease are not amenable to biopsy and/or in vivo functional assessment, alternative approaches are needed. The aim of this research was to provide a case study in which assessment of reprogrammed iPS cells from a patient skin biopsy could be used to diagnose the molecular genetics of hard-to-solve variants in known genetic diseases.

In this study, the fate of unsolved variants was determined by gene expression in dRPE cells, one of two clinically relevant cells types with disease-specific pathogenesis in Stargardt disease in three patients with a single solved allele. Variants of the *ABCA4* gene did not disadvantage fibroblast growth, dedifferentiation into iPS cells or reprogramming into dRPE cells, which were grossly normal for growth and maturation, with similar morphological characteristics and metabolism but altered levels of *ABCA4* transcripts compared with controls (Kady, N., et al. IOVS 2018;59:ARVO E-Abstract 3045; Radu, R., et al. IOVS 2019;60:ARVO E-Abstract 2343; Hu, J., et al. IOVS 2020:61:ARVO E-Abstract 1507). These results suggested the unknown variants in all three patients occur in important promoter or splice sequences, which was validated in two patients during the course of this study.[4]

Attributing expression levels to disease causality and severity through in vitro assays or animal models provides important insights but often assesses single alleles and lacks the insight of a complex genetic background.[4,29–32] Patient-derived cells are

likely to more closely reflect the splicing and editing events occurring in patients. Conserved expression and correct splicing of some normal transcripts from all splice variant alleles was observed. Three splice variants previously categorized as severe based on loss of expression in midi-gene assays[4] exhibited higher expression in cultured dRPE cells. The c.5461-10T>C splice variant had reduced but detectable expression and the c.570+1798A>G splice variant had approximately a quarter the normal expression levels compared to 0% wild type RNA in a midi-gene assay, indicating both splice variants undergo some nonsense mediated mRNA decay (NMD). By contrast, the c.2654-8T>G splice variant accounted for approximately half the expected expression of the ref allele compared to 13% WT RNA in the midi-gene assay. Two of the three independent S dRPE samples show total *ABCA4* expression similar to control, whereas S2 has greatly increased expression, with the relative level of each allele is consistent. Minimally, this example well illustrates the need to study multiple independently generated lines from each patient. These alterations are possibly due to trans-acting upregulation as the missense allele is also overexpressed, which may be in response to low or defective protein function or to another as-yet unidentified variant in promoter or enhancer regions. Finally, consideration must be given to the atypical culture environment, the age of the cells in culture and directed reprogramming of iPS to dRPE cells.

Allele specific imbalance allows individualization of alleles at the non-matched nucleotides of disease-causing variant to probe whether missense, non-sense and destabilizing variants undergo NMD resulting in unequal expression of the two alleles, thereby inferring variant severity. Twenty-eight percent expression of the normal allele is sufficiently low to cause mild disease as seen in the patient with two likely splice variants. Eleven percent expression of the normal allele in the presence of the R1129L variant causes moderate disease that may be attributable to lower expression of the normal allele combined with the decreased expression and dysfunction of the missense allele.[31] By contrast, 46% expression of the normal allele in the presence of E1122K causes moderate-to-severe disease, indicating clear dissociation between protein function and stability to disease severity. The variability in transcript levels from multiple lines of the same patient can limit our ability to make correlations to the patient's clinical disease severity, indicating the need to assess multiple independent patient-derived lines. Together, these data support the common understanding that NMD can be less debilitating than variants that alter protein structure and function.

The patient missense variants occur in the ATP Nucleotide Binding Domain 1 (NBD1) and not NBD2, which is required for ATP hydrolysis. Variants in the carboxyterminal end of NBD1 have decreased expression in an exogenous system (R1129L), decreased nucleotide binding or activity (A1038V, G1091E, and R1129L), as well as differences in retinoid binding (A1038V and G1091E).[31,33] Although many NBD1 variants are classified as "intermediate" or "moderate" in severity (G863A, R1108C, and P1180L), others are classified as "severe" or "null-like" (E1022K and E1087K), clearly indicating the degree to which individual variants disrupt protein structure and function is the critical feature. In this study, E1122K and R1129L can both be classified as severe as the expression of 46% and 11% normal transcript is insufficient to overcome the deficit of the mutated proteins, respectively, with the caveat that the expression level of the normal transcript from the splice variants might be reduced or increased in vivo as a result of aging or other factors.

The transcriptomes of the patient's dRPE cells implicate oxidative and endoplasmic reticulum stress, both consistent with disease phenotypes, as well as a broad range of biological functions likely representative of multifaceted reactive responses rather than primary alterations due to the *ABCA4* variants. With the limited number of patient and controls analyzed, pathway interpretation should be considered limited. Statistical analyses suggest that a minimum of 10 patient lines and additional control lines would be needed to generate reliable insights. In this limited dataset, genes in the UPR pathway were upregulated in all patient lines, suggesting improper folding, and membrane mislocalization of both missense and splice variants. Upregulation of the UPR in the patient line with two splice variants further suggests that aberrantly spliced polypeptides are likely produced although short-lived in the endoplasmic reticulum, although it should be noted that only a small number of UPR genes were affected. Consequently, patients with two splice variants may have increased potential to benefit from gene therapy avoiding immune sensitization from exogenous expression and from small molecule therapy as they lack structurally abnormal protein.

PCA of the dRPE transcriptomes clustered the three distinct patients together and separate from the control, suggesting that although genetic background differences could account for some DEGs, the shared DEGs are primarily driven by mutations in *ABCA4*. Even within this limited set of patient samples, both patient-specific and disease-specific transcriptome alterations may be idiosyncratic to the cell lines or

result from patient-specific *ABCA4* variants and other personal genetic contributions. Clear dissociation of individual versus general transcriptomic responses to *ABCA4* pathological variants would require additional patient dRPE cells, while also considering aging of the dRPE and its environment. For example, one of the dRPE cells in this study showed specific biochemical, morphological, and functional changes in aged cultures, recapitulating key RPE phenotypic features of the Stargardt mouse model[34–36] and when challenged with oxidative stress or by rod photoreceptor outer segments that are phagocytosed by dRPE (unpublished data, N. Kady, IOVS, 2018; 59(9):4502; R. Radu, IOVS, 2019;60(9):2343; J. Hu, IOVS, 2020:61(7):1507). Similarly, specific aspects of disease may be contributed by different biological demands of *ABCA4* in different cell types, for example in dRPE versus photoreceptor precursor cells. Last, emergent phenotypes due to the close relationship between these two cell types may not be apparent in single-cell type cultures but may be revealed in retinal organoid-RPE co-cultures.[37,38]

In conclusion, patient-specific molecular analysis can aid in the molecular genetics of hard to solve genetic diseases. This is particularly relevant for diseases manifesting in tissues that are difficult or deleterious to biopsy, such as the central nervous system or retina, and in diseases in which variants may be in "dark DNA" or other poorly accessed genomic loci. The ability to reprogram patient-derived iPS cells into the pathophysiologically susceptible specific cell types provides a window into the nature of unsolved variants, sets the stage for variant discovery, and traverses the critical boundaries of translational research that will enable more patients to participate in and benefit from clinical trials and their emergent therapies.

Acknowledgments

The authors thank the Daljit S. and Elaine Sarkaria Charitable Foundation for their generous support, as well as the patient participants, without whom this work would not be possible.

Funded by the Daljit S. and Elaine Sarkaria Charitable Foundation (M.B.G. and R.A.R.), Eli and Edythe Broad Center of Regenerative Medicine and Stem Cell Research Rose Hills Foundation Innovator Grant (R.A.R.), R01EY025002 from the National Institutes of Health (NIH; R.A.R.), EY000331 Core Grant from the NIH for Vision Research at UCLA Stein Eye Institute, Research to Prevent Blindness unrestricted grant to the Department of Ophthalmology at UCLA Stein Eye Institute, and R01EY022356, R01EY018571, and S10OD023469 from the NIH (R.C.). The funding organizations had no role in the design or conduct of this research.

Author Contributions: Conceptualization: A.M., R.C., and M.B.G. Data curation: A.M., R.A.R., and R.C. Formal analysis: A.M., S.S., J.W., S.K., and R.C. Funding acquisition: R.A.R., R.C., and M.B.G. Investigation: A.M., J.W., S.K., Y.L., X.Q., Z.J., and J.H. Methodology: A.M., J.W., S.K., R.C. Resources: A.M., A.D., S.S., R.A.R., R.C., and M.B.G. Project administration: A.M. and R.C. Supervision: A.M., R.A.R., R.C., and M.B.G. Validation: A.M., R.A.R., and R.C. Visualization: A.M., Z.J., J.W., S.K., and R.C. Writing—original draft preparation: A.M. Writing—review and editing: A.M., M.B.G., R.C., R.A.R., J.W., and S.K. All authors have read and agreed to the published version of the manuscript.

Disclosure: **A. Matynia,** None; **J. Wang,** None; **S. Kim,** None; **Y. Li,** None; **A. Dimashkie,** None; **Z. Jiang,** None; **J. Hu,** None; **S.P. Strom,** None; **R.A. Radu,** None; **R. Chen,** None; **M.B. Gorin,** None

References

1. Mansfield BC, Yerxa BR, Branham KH. Implementation of a registry and open access genetic testing program for inherited retinal diseases within a non-profit foundation. *Am J Med Genet C Semin Med Genet*. 2020;184:838–845, doi:10.1002/ajmg.c.31825.
2. de Bruijn SE, Fadaie Z, Cremers FPM, Kremer H, Roosing S. The Impact of Modern Technologies on Molecular Diagnostic Success Rates, with a Focus on Inherited Retinal Dystrophy and Hearing Loss. *Int J Molec Sci*. 2021;22:2943.
3. Zampaglione E, Kinde B, Place EM, et al. Copy-number variation contributes 9% of pathogenicity in the inherited retinal degenerations. *Genet Med*. 2020;22:1079–1087.
4. Khan M, Cornelis SS, Pozo-Valero MD, et al. Resolving the dark matter of ABCA4 for 1054 Stargardt disease probands through integrated genomics and transcriptomics. *Genet Med*. 2020;22:1235–1246.
5. Braun TA, Mullins RF, Wagner AH, et al. Non-exomic and synonymous variants in ABCA4 are an important cause of Stargardt disease. *Hum Mol Genet*. 2013;22:5136–5145.

6. Allikmets R, Singh N, Sun H, et al. A photoreceptor cell-specific ATP-binding transporter gene (ABCR) is mutated in recessive Stargardt macular dystrophy. *Nat Genet*. 1997;15:236–246.
7. Cremers FPM, Lee W, Collin RWJ, Allikmets R. Clinical spectrum, genetic complexity and therapeutic approaches for retinal disease caused by ABCA4 mutations. *Prog Retin Eye Res*. 2020;79:100861.
8. Sangermano R, Garanto A, Khan M, et al. Deep-intronic ABCA4 variants explain missing heritability in Stargardt disease and allow correction of splice defects by antisense oligonucleotides. *Genet Med*. 2019;21:1751–1760.
9. Nassisi M, Mohand-Said S, Andrieu C, et al. Prevalence of ABCA4 Deep-Intronic Variants and Related Phenotype in An Unsolved "One-Hit" Cohort with Stargardt Disease. *Int J Mol Sci*. 2019;20:5053.
10. Zernant J, Lee W, Collison FT, et al . Frequent hypomorphic alleles account for a significant fraction of ABCA4 disease and distinguish it from age-related macular degeneration. *J Med Genet*. 2017;54:404–412.
11. Lenis TL, Hu J, Ng SY, et al. Expression of ABCA4 in the retinal pigment epithelium and its implications for Stargardt macular degeneration. *Proc Natl Acad Sci USA*. 2018;115:E11120–E11127.
12. Illing M, Molday LL, Molday RS The 220-kDa rim protein of retinal rod outer segments is a member of the ABC transporter superfamily. *J Biol Chem*. 1997;272:10303–10310.
13. Sangermano R, Khan M, Cornelis SS, et al. ABCA4 midigenes reveal the full splice spectrum of all reported noncanonical splice site variants in Stargardt disease. *Genome Res*. 2018;28:100–110.
14. Schulz HL, Grassmann F, Kellner U, et al. Mutation Spectrum of the ABCA4 Gene in 335 Stargardt Disease Patients From a Multicenter German Cohort-Impact of Selected Deep Intronic Variants and Common SNPs. *Invest Ophthalmol Vis Sci*. 2017;58:394–403.
15. Fadaie Z, Khan M, Del Pozo-Valero M, et al . The Abca Study, G. Identification of splice defects due to noncanonical splice site or deep-intronic variants in ABCA4. *Hum Mutat*. 2019;40:2365–2376.
16. Choudhary P, Booth H, Gutteridge A, et al . Directing Differentiation of Pluripotent Stem Cells Toward Retinal Pigment Epithelium Lineage. *Stem Cells Transl Med*. 2017;6:490–501.
17. Hazim RA, Karumbayaram S, Jiang M, et al. Differentiation of RPE cells from integration-free iPS cells and their cell biological characterization. *Stem Cell Res Ther*. 2017;8:217.
18. Reichman S, Terray A, Slembrouck A, et al . From confluent human iPS cells to self-forming neural retina and retinal pigmented epithelium. *Proc Natl Acad Sci USA*. 2014;111:8518–8523.
19. Okamoto S, Takahashi M. Induction of retinal pigment epithelial cells from monkey iPS cells. *Invest Ophthalmol Vis Sci*. 2011;52:8785–8790.
20. Kim J, Koo BK, Knoblich JA. Human organoids: model systems for human biology and medicine. *Nat Rev Mol Cell Biol*. 2020;21:571–584.
21. Cowan CS, Renner M, De Gennaro M, et al. Cell Types of the Human Retina and Its Organoids at Single-Cell Resolution. *Cell*. 2020;182:1623–1640.e1634.
22. Gao ML, Lei XL, Han F, et al . Patient-Specific Retinal Organoids Recapitulate Disease Features of Late-Onset Retinitis Pigmentosa. *Front Cell Dev Biol*. 2020;8:128.
23. Blenkinsop TA, Saini JS, Maminishkis A, et al. Human Adult Retinal Pigment Epithelial Stem Cell-Derived RPE Monolayers Exhibit Key Physiological Characteristics of Native Tissue. *Invest Ophthalmol Vis Sci*. 2015;56:7085–7099.
24. Jha BS, Bharti K. Regenerating Retinal Pigment Epithelial Cells to Cure Blindness: A Road Towards Personalized Artificial Tissue. *Curr Stem Cell Rep*. 2015;1:79–91.
25. Meyer JS, Howden SE, Wallace KA, et al. Optic vesicle-like structures derived from human pluripotent stem cells facilitate a customized approach to retinal disease treatment. *Stem Cells*. 2011;29:1206–1218.
26. Tucker BA, Mullins RF, Streb LM, et al . Patient-specific iPSC-derived photoreceptor precursor cells as a means to investigate retinitis pigmentosa. *Elife*. 2013;2:e00824.
27. Buchholz DE, Pennington BO, Croze RH, Hinman CR, Coffey PJ, Clegg DO. Rapid and efficient directed differentiation of human pluripotent stem cells into retinal pigmented epithelium. *Stem Cells Transl Med*. 2013;2:384–393.
28. Runhart EH, Sangermano R, Cornelis SS, et al. The Common ABCA4 Variant p.Asn1868Ile Shows Nonpenetrance and Variable Expression of Stargardt Disease When Present in trans With Severe Variants. *Invest Ophthalmol Vis Sci*. 2018;59:3220–3231.
29. Trezza A, Bernini A, Langella A, et al. A Computational Approach From Gene to Structure Analysis of the Human ABCA4 Transporter Involved in Genetic Retinal Diseases. *Invest Ophthalmol Vis Sci*. 2017;58:5320–5328.

30. Zhong M, Molday LL, Molday RS. Role of the C terminus of the photoreceptor ABCA4 transporter in protein folding, function, and retinal degenerative diseases. *J Biol Chem*. 2009,284:3640–3649.
31. Sun H, Smallwood PM, Nathans J. Biochemical defects in ABCR protein variants associated with human retinopathies. *Nat Genet*. 2000;26:242–246.
32. Sun H, Nathans J. ABCR: rod photoreceptor-specific ABC transporter responsible for Stargardt disease. *Methods Enzymol*. 2000;315:879–897.
33. Garces F, Jiang K, Molday LL, et al . Correlating the Expression and Functional Activity of ABCA4 Disease Variants With the Phenotype of Patients With Stargardt Disease. *Invest Ophthalmol Vis Sci*. 2018;59:2305–2315.
34. Radu RA, Hu J, Yuan Q, et al . Complement system dysregulation and inflammation in the retinal pigment epithelium of a mouse model for Stargardt macular degeneration. *J Biol Chem*. 2011;286:18593–18601.
35. Radu RA, Mata NL, Bagla A, Travis GH. Light exposure stimulates formation of A2E oxiranes in a mouse model of Stargardt's macular degeneration. *Proc Natl Acad Sci USA*. 2004;101:5928–5933.
36. Kady N, Hu J, Jiang Z, Gorin MB, Matynia A, Radu RA Membrane Attack Complex Mediates Retinal Pigment Epithelium Cell Death in Stargardt Disease. In preparation.
37. Ghareeb AE, Lako M, Steel DH. Coculture techniques for modeling retinal development and disease, and enabling regenerative medicine. *Stem Cells Transl Med*. 2020;9:1531–1548.
38. Akhtar T, Xie H, Khan MI, et al . Accelerated photoreceptor differentiation of hiPSC-derived retinal organoids by contact co-culture with retinal pigment epithelium. *Stem Cell Res*. 2019;39:101491.